



Pressure effects in CeNi

A. Mirmelstein^{a,*}, E. Clementyev^a, O. Kerbel^a, D. Kozlenko^b, Yu. Akshentsev^c, V. Voronin^c, I. Berger^c

^a Department of Experimental Physics, Russian Federal Nuclear Center – E.I. Zababakhin Institute of Technical Physics, Vasil'ev Street 13, Snezhinsk, 456770 Chelyabinsk Region, Russia

^b I.M. Frank Laboratory of Neutron Physics, JINR, Dubna 141980, Russia

^c Institute for Metal Physics, Russian Academy of Sciences, 620041 Ekaterinburg, Russia

A B S T R A C T

Magnetic susceptibility of the intermediate-valence CeNi compound was measured under external pressure of 0.8, 1.05 and 1.25 GPa. The results obtained extend the pressure–temperature phase diagram of CeNi up to $P = 2$ GPa and $T = 300$ K. It is shown that the pressure-induced phase of CeNi has a tetragonal symmetry. Specific heat measurements for the $Ce_{1-x}La_xNi$ –CeNi– $Ce_{1-x}Lu_xNi$ series demonstrate significant increase of the f -electron hybridization due to chemical pressure.

© 2008 Elsevier B.V. All rights reserved.

1. Introduction

Plutonium and cerium are distinguished among the other elements of the periodic table because of their anomalous physical properties including unusual structural phase transitions accompanied by the f -electron collapse and volume discontinuity. The nature of these transitions is not understood completely, however similar character of the $4f$ and $5f$ electrons encourages joint study of phase transition mechanisms in Pu, Ce and their compounds. Low temperature bulk properties and a degree of the f -electron shell delocalization of the intermediate-valence compound CeNi remind the properties of metallic plutonium [1]. Moreover, CeNi undergoes a pressure-induced first-order volume-collapse phase transition [2]. Thus, CeNi is an attractive model system to study the mechanisms of phase transformations resulting from the f -electron instability and strong electron correlations [3].

In the present paper we present the extended pressure–temperature phase diagram of CeNi and the results of specific heat study of chemical pressure effects in the CeNi system.

2. Results and discussion

2.1. Pressure–temperature phase diagram of CeNi

CeNi has the CrB-type orthorhombic crystal structure (space group $Cmcm$) with the room-temperature lattice parameters $a = 3.786$ Å, $b = 10.548$ Å, $c = 4.363$ Å. Although at ambient pressure CeNi displays clear signatures of lattice instability upon cooling [4,5], structural transformations do not occur down to the lowest temperature. In 1985 Gignoux and Voiron demonstrated the exist-

tence of a pressure-induced volume-collapse first-order phase transition in CeNi and determined its phase P – T diagram up to 0.5 GPa and 150 K [2]. Recently, the room-temperature first-order transition was observed at $P \sim 2$ GPa by neutron diffraction technique [3]. To fill in the pressure gap $0.5 < P < 2$ GPa and to bridge the neutron diffraction results to the earlier established P – T phase diagram of CeNi we measured the temperature dependence of the CeNi magnetic susceptibility under quasi-hydrostatic pressure up to 1.25 GPa. Sample preparation and characterization are described in [3]. The cast polycrystalline sample (mass ~ 40 mg) was placed in a Cu–Be clamp-type pressure-cell and fluorinert was used as the pressure transmitted medium. Magnetic susceptibility was measured with Quantum Design Physical Properties Measurement System (QD PPMS) by the DC technique in a magnetic field of 3 T. At low temperatures ~ 7 K the pressure was calibrated from the pressure dependence of the superconducting transition temperature of Pb (DC measurements at a field of 20 Oe). We obtained a linear relation between pressure at ~ 7 K (P_{7K}) and pressure P_{300K} applied at room temperature. The temperature dependences of magnetic susceptibility of CeNi at applied pressure $P_{300K} = 0.8, 1.05$ and 1.25 GPa exhibit a significant thermal hysteresis associated with the first-order structural phase transition (Fig. 1). The hysteresis is very large as compared with the 25–30 K temperature hysteresis observed for the CeNi single crystal [2]. The broadening may be connected with polycrystalline character of our sample and also with continuous pressure variation in the pressure cell with temperature. The latter results from the high thermal expansion coefficient of CeNi and the strong volume change (of the order of a few percent) due to the phase transition itself. The transition temperature T_{tr} can be determined as a temperature of the maximum of the difference curve $\Delta\chi(T) = \chi_{cooling}(T) - \chi_{heating}(T)$ (the inset in Fig. 1). The transition pressure P_{tr} can be estimated by the linear interpolation between P_{7K} and P_{300K} to T_{tr} . Fig. 2 shows that (P_{tr}, T_{tr}) points obtained by this procedure correspond to the empirical

* Corresponding author. Tel./fax: +7 35146 52070.

E-mail address: mirmelstein@mail.ru (A. Mirmelstein).

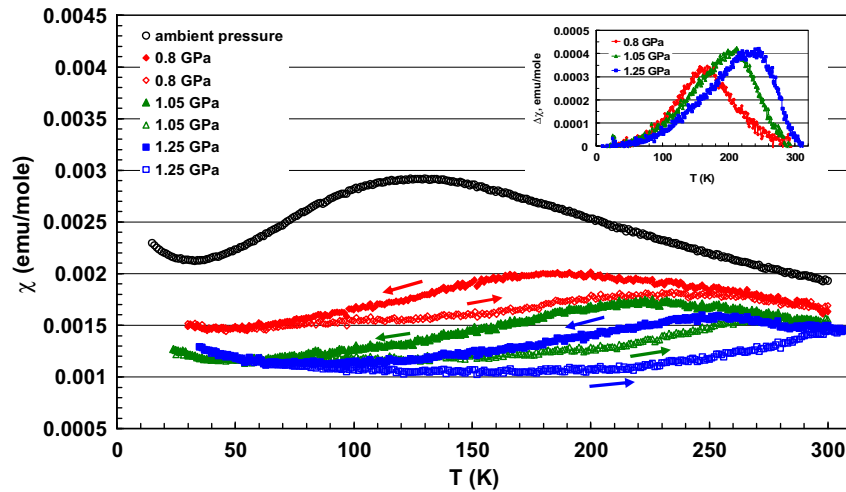


Fig. 1. The temperature dependence of magnetic susceptibility of CeNi measured at ambient pressure and under applied pressure $P_{300\text{ K}} = 0.8, 1.05, \text{ and } 1.25$ GPa. Arrows indicate the temperature direction. The inset shows the difference $\Delta\chi(T) = \chi_{\text{cooling}}(T) - \chi_{\text{heating}}(T)$ curves vs. temperature.

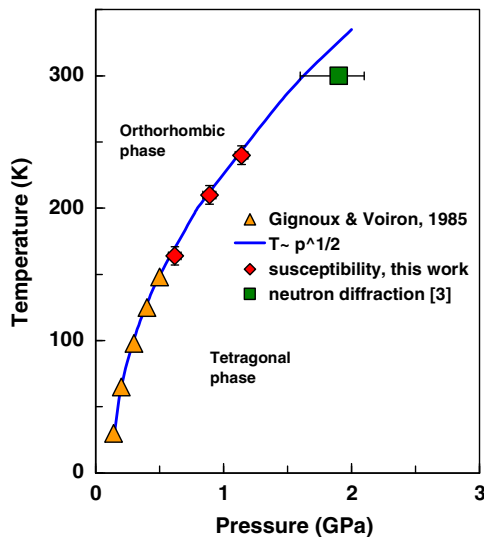


Fig. 2. P - T diagram of ambient-pressure orthorhombic and pressure-induced tetragonal phases in CeNi.

$T_{\text{tr}} \sim P_{\text{tr}}^{1/2}$ dependence established by Gignoux and Voiron [2]. The room-temperature point (300 K, ~ 2 GPa) deduced from the neutron diffraction data seems also to belong to the same phase border line. In this case this line turns out to be the only phase transition line at $P < 2$ GPa and $T < 300$ K.

In the previous paper [3] we suggested the symmetry of the pressure-induced phase to be higher than that of the orthorhombic ambient-pressure CeNi structure. In fact, the diffraction pattern of CeNi at 5 GPa correspondent to the pure high-pressure phase [3] can be described in terms of the tetragonal symmetry with the crystal lattice parameters $a = 3.748$ Å and $c = 5.796$ Å (Fig. 3, upper panel). However, it is not excluded that slightly better description is achieved by doubling the c parameter, i.e. with $a = 3.748$ Å and $c = 2 \times 5.796 = 11.592$ Å (Fig. 3, lower panel). While the high-pressure phase space group is not determined yet, the deduced values of the lattice parameters allow to estimate the volume jump $\Delta V/V$ due to the room-temperature pressure-induced transition, $\Delta V/V = [V_{300\text{ K}}(P=0) - V_{300\text{ K}}(5\text{ GPa})] / V_{300\text{ K}}(P=0) = 6.5\%$.

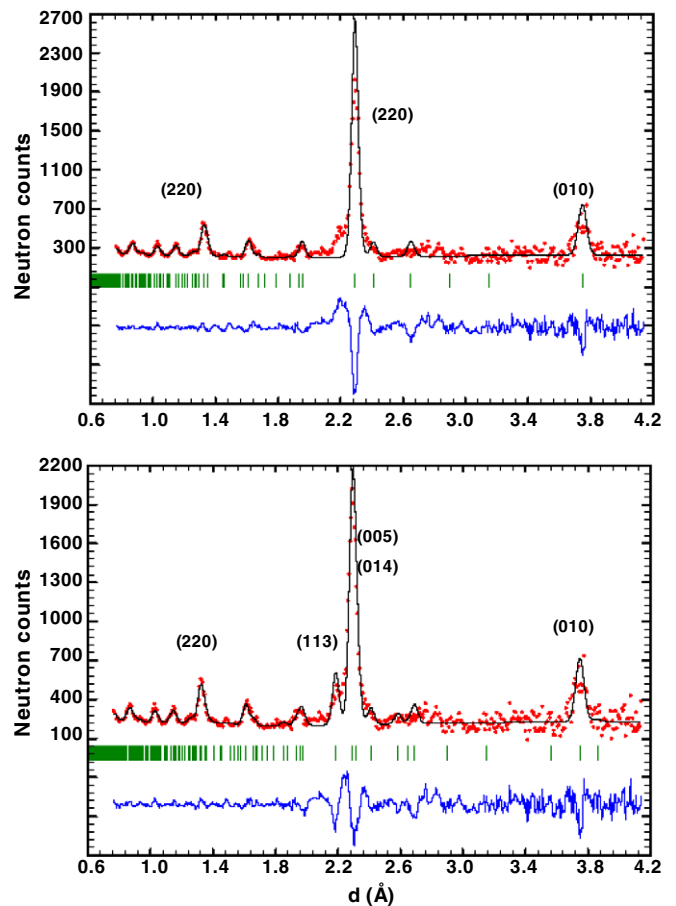


Fig. 3. The neutron diffraction pattern of CeNi at $P = 5$ GPa and $T = 300$ K (points) [3]. Solid line shows the calculated pattern assuming tetragonal crystal lattice symmetry with the lattice parameters $a = 3.748$ Å, $c = 5.796$ Å (upper panel) and $a = 3.748$ Å, $c = 2 \times 5.796 = 11.592$ Å (lower panel). hkl Miller indexes are indicated for the most intensive reflections.

2.2. Specific heat study of chemical pressure effects in CeNi

In order to study the chemical pressure effects on the properties of the intermediate-valence CeNi specific heat of $\text{Ce}_{1-x}\text{La}_x\text{Ni}$

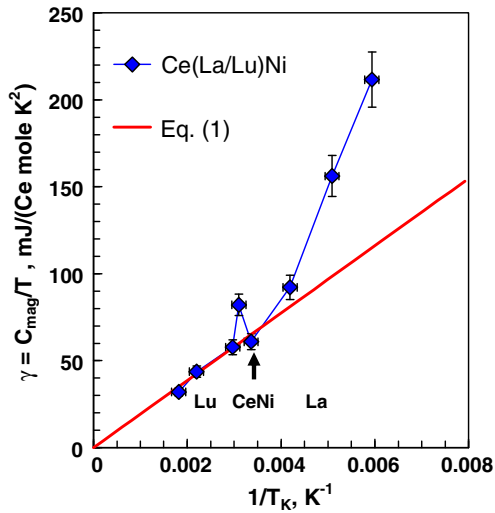


Fig. 4. Sommerfeld coefficient $\gamma = C_{\text{mag}}(T)/T_{T \rightarrow 0}$ as a function of the inverse Kondo temperature T_K for $\text{Ce}_{1-x}\text{La}_x\text{Ni}$ ($x = 0.4, 0.2, 0.1$), CeNi and $\text{Ce}_{1-x}\text{Lu}_x\text{Ni}$ ($x = 0.05, 0.1, 0.2, 0.4$) derived from the specific heat measurements. T_K is determined as described in the text and the solid line represents the slope calculated with Eq. (1) (see text for details).

($x = 0.4, 0.2, 0.1$), CeNi , $\text{Ce}_{1-x}\text{Lu}_x\text{Ni}$ ($x = 0.05, 0.1, 0.2, 0.4$) series was measured in the temperature range $2 < T < 300$ K by the relaxation technique using QD PPMS. The magnetic contribution $C_{\text{mag}}(T)$ to the specific heat was determined by subtracting the LaNi specific heat from the $C(T)$ curves of the samples. The results obtained show an upward shift of the temperature of the maximum T_{max} of $C_{\text{mag}}(T)$ curves and a decrease of the Sommerfeld coefficient $\gamma = C_{\text{mag}}(T)/T_{T \rightarrow 0}$ under increase of the chemical pressure induced by the Ce substitutions for La and the Lu substitutions for Ce. Theoretical approaches predict the Sommerfeld coefficient in the Kondo-systems to be proportional to the fractional f -orbital occupation $\langle n_f \rangle$ and inversely proportional to the Kondo temperature T_K (here $T_K = E_0/k_B$, where E_0 is the characteristic energy scale) [6,7]:

$$\gamma = C_{\text{el}}/T_{T \rightarrow 0} = N_A \pi^2 k_B^2 \langle n_f \rangle \frac{1}{3k_B T_K} \frac{N-1}{N}, \quad (1)$$

where N_A is the Avogadro number, k_B is the Boltzmann constant, N is the f -shell effective magnetic degeneracy (for Ce^{3+} $J = 5/2$ and $N = 6$), and the Kondo temperature T_K correlates with T_{max} , namely, $T_{\text{max}}/T_K \approx 0.35$ [6]. Fig. 4 shows that at least for the $\text{Ce}_{1-x}\text{Lu}_x\text{Ni}$ series (excluding $\text{Ce}_{0.95}\text{Lu}_{0.05}\text{Ni}$) γ varies proportionally to $1/T_K$, in agreement with Eq. (1). For a comparison Fig. 4 shows the theoretical slope of γ vs. $1/T_K$ dependence, which is calculated for CeNi with

Eq. (1), assuming $\langle n_f \rangle = 0.85$ (corresponding to the effective Ce valence 3.15 [4]), the magnetic degeneracy $N = 6$, and $T_K \approx T_{\text{max}}/0.35 = 298$ K, where $T_{\text{max}} = 106$ K is the temperature of the maximum of the CeNi $C_{\text{mag}}(T)$ curve. Note, that this value of T_K is in fairly good agreement with the characteristic energy scale $E_0 = 25.7$ meV (≈ 298 K) for CeNi derived from the inelastic neutron scattering experiments [8]. Thus, according to our data, the chemical compression of CeNi increases the f -electron hybridization, as follows from increase of T_K . It is worth mentioned that the magnetic degeneracy of the f -states should be taken into account for a correct calculation of the Sommerfeld coefficient for valence-fluctuating systems [6,7].

3. Conclusion

The pressure–temperature phase diagram of CeNi is extended up to $P = 2$ GPa and $T = 300$ K. It is shown that only two CeNi phases exist within this P – T domain ($P \leq 2$ GPa, $T \leq 300$ K), namely, the ambient-pressure orthorhombic CrB -type structure and the high-pressure phase of the tetragonal symmetry. The volume jump at the room-temperature structural transition is estimated to be 6.5%. The specific heat measurements revealed no signature of ambient-pressure phase transitions in the chemically compressed $\text{Ce}_{1-x}\text{Lu}_x\text{Ni}$ compositions. Analysis of the specific heat curves for the $\text{Ce}_{1-x}\text{La}_x\text{Ni}$ – CeNi – $\text{Ce}_{1-x}\text{Lu}_x\text{Ni}$ series shows the chemical pressure-induced increase of the Kondo temperature and the correspondent decrease of the Sommerfeld coefficient.

Acknowledgements

This work was performed under auspices of the State Corporation ‘Rosatom’ (State Contract # H.06.4.1.47.03.08.124). Financial support by RFBR (Grant No. # 05-08-33456-a) is gratefully acknowledged.

References

- [1] E. Clementyev, A. Mirmelstein, P. Böni, J. Alloys Comp. 444&445 (2007) 292.
- [2] D. Gignoux, J. Voiron, Phys. Rev. B 32 (1985) 4822; D. Gignoux, C. Vettier, J. Voiron, JMMM 70 (1987) 388.
- [3] A. Mirmelstein, E. Clementyev, V. Voronin, Yu. Akshentsev, D. Kozlenko, A. Kutepov, A. Petrovtsev, Yu. Zuev, J. Alloys Comp. 444&445 (2007) 281.
- [4] V.N. Lazukov, E.V. Nefedova, V.V. Sikolenko, U. Staub, P.A. Alekseev, M. Braden, K.S. Nemkovskii, C. Pradervant, I.P. Sadikov, L. Soderholm, N.N. Tiden, Appl. Phys. A 74 (Suppl.) (2002) S559.
- [5] E.S. Clementyev, P.A. Alekseev, M. Braden, J.-M. Mignot, G. Lapertot, V.N. Lazukov, I.P. Sadikov, Phys. Rev. B 57 (2000) R8099.
- [6] N.E. Bickers, D.L. Cox, J.W. Wilkins, Phys. Rev. B 36 (1987) 2036.
- [7] M. Loewenhaupt, K.H. Fischer, in: K.H.J. Buschow (Ed.), Handbook of Magnetic Materials, Elsevier Science Publishing, 1993, pp. 503–609. Chapter 6.
- [8] E. Clementyev, J.-M. Mignot, P.A. Alekseev, V.N. Lazukov, E.V. Nefedova, I.P. Sadikov, M. Braden, R. Kahn, G. Lapertot, Phys. Rev. B 61 (2000) 6189.